Rapid evolution of fine-scale recombination during domestication

Zheng-Xi Liu [1,2,3,†], Ming Li [4,†], Si Si [1,2], Jian-Hai Chen [5], Li-Rong Hu [1,2], Min-Sheng Peng [1,2], Ting-Ting Yin [1,2], Ali Esmailizadeh [1,2,6], Chang Zhang [1,2], Lu-Jiang Qu [7], Xue-Mei Lu[1], Jian-Lin Han [8,*], Ya-Ping Zhang[1,2,9,*], Ming-Shan Wang [1,2,3,*]

1. Key Laboratory of Genetic Evolution & Animal Models, State Key Laboratory of Genetic Resources and Evolution, Kunming Institute of Zoology, Chinese Academy of Sciences, Kunming 650201, P. R. China
2. Yunnan Laboratory of Molecular Biology of Domestic Animals, Kunming Institute of Zoology, Chinese Academy of Sciences, Kunming 650201, P. R. China
3. Kunming College of Life Science, University of Chinese Academy of Sciences, Kunming, P. R. China
4. Zoology and Evolutionary Biology, Department of Biology, University of Konstanz, Konstanz, Germany
5. Department of Ecology and Evolution, The University of Chicago, Chicago, IL 60637
6. Department of Animal Science, Faculty of Agriculture, Shahid Bahonar University of Kerman, 76169-133, Kerman, PB, Iran
7. National Engineering Laboratory for Animal Breeding, Department of Animal Genetics and Breeding, College of Animal Science and Technology, China Agricultural University, Beijing 100193, P. R. China
8. Yazhouwan National Laboratory, Sanya 572024, P. R. China
9. State Key Laboratory for Conservation and Utilization of Bio-resource, Yunnan University, Kunming 650091, P. R. China

† These authors contributed equally to this work
* Corresponding authors
Ming-Shan Wang: wangmingshan@mail.kiz.ac.cn
Ya-Ping Zhang: zhangyp@mail.kiz.ac.cn
Jian-Lin Han: hanjianlin@yzwlab.cn

ABSTRACT

Recombination serves as a central force driving the evolution of genomic diversity in sexually reproducing organisms. Despite its fundamental role, the evolutionary dynamics of recombination rates remain largely elusive. The domestication of animals, characterized by dynamic selective pressures, provides a unique lens through which to investigate these phenomena. Here, we constructed a fine-scale recombination map using whole-genome data from domestic chickens, including both contemporary commercial breeds and their wild progenitor, the Red Junglefowl (RJF). Our analysis reveals a rapid evolution of the recombination landscape within and between chicken populations, and we find that the average recombination rate decreased during chicken domestication. Remarkably, this trend is further corroborated by re-analysis of the genomes of several domestic species including ducks, goats, pigs, and sheep. Contrary to the hypothesis that domestication leads to an increase in recombination rates, our results provide no support for such a scenario. We suggest that a low recombination rate is beneficial for maintaining uniform and stable phenotypes in domestic breeds during selective inbreeding. Furthermore, we find significant variation in recombination hotspots across chicken populations, which is particularly pronounced in commercial breeds despite their recent divergence. The rapid turnover of recombination hotspots and coldspots appears to be closely linked to selective sweeps. Interestingly, in contrast to prevailing observations in most species, we find that long-term selective inbreeding results in a negative correlation between recombination rates and the frequency of introgressed ancestry from other RJF subspecies. Our results provide insights into the complex interplay of evolutionary forces shaping the evolution of recombination.

Keywords: recombination rate, introgression, domestication, genome sequencing

INTRODUCTION

Meiotic recombination is a crucial process in which DNA exchange occurs between homologous chromosomes, ensuring their accurate segregation in sexually reproducing species. This process is central to generating and maintaining genetic diversity, facilitating the development of novel haploid gametes. Empirical evidences reveal that recombination serves as a major force in both micro- and macroevolutionary processes [1, 2], driving the formation of new combinations of alleles and haplotypes. This enables the efficiency of adaptive evolution and selection, highlighting its practical and fundamental significance. Investigating the recombination landscape provides insights into how recombination influences the selection, evolution, and demographic history of populations. Moreover, it allows for a broader exploration of the mechanisms and forces shaping the evolution of genomes and species [3-5]. Practically, manipulating the recombination rate has practical implications, potentially enhancing the efficiency of the breeding processes [6, 7].

Influenced by demographic, environmental, and genetic factors [8-11], the recombination rate is not static but exhibits high variation across taxa, populations, and individuals, even within chromosomes[8, 12]. This rate is unevenly distributed across the genome in many species, with higher rates found predominantly located at the distal ends of chromosomes, termed "hotspots", and lower rates (coldspots) found in the pericentromere [2]. These hotspots are typically 1-2kb in size [2]. In mice and humans, the position of the hotspot is largely determined by *PRDM9*, a zinc-finger protein that binds to specific DNA motifs [13]. However, the binding domain of *PRDM9* evolves rapidly, and hotspot regions show a rapid turnover [10, 14-16]. Despite lacking functional *PRDM9*, species like birds, canids and yeast maintain recombination patterns and hotspots [17-19]. The locations of recombination hotspots tend to occur at promoters or near transcription start sites (TSSs), remaining highly stable over evolutionary time [20]. However, the molecular basis influencing the distribution and occurrence of recombination events is poorly understood in many organisms, particularly those lacking functional *PRDM9*.

Recombination can influence the efficacy of selection, and reciprocally, it can be influenced by episodes of selection [21]. Domestication is a long-term experiment by humans with animals and plants over thousands of years, involving intense selection and breeding for targeted traits that have shaped the genetic architecture and physiological and phenotypic diversity of domesticated species. This provides a unique opportunity to investigate the interplay between the selection and recombination. However, existing studies have yielded inconsistent and sometimes contradictory results. Some suggested an overall increase in recombination rates during domestication, positing that selection generally favors increased recombination during periods of rapid evolutionary change [22, 23]. While others argue that higher recombination is a preadaptation to domestication. In this view, a population with a higher recombination rate would increase its efficiency and responsiveness to the selection, making it more likely to be successfully domesticated [24]. Additionally, Lenormand and colleagues proposed that a reduced recombination rate in domesticates may confer benefits by protecting against maladaptive gene flow from wild relatives [25].

The evolution of recombination rates through domestication remains a topic of debate, with most genome-wide comparisons focused on plant species rather than animals. Animal domestication episodes and processes may differ from those in plants [26, 27]. Previous investigations into the relationship between recombination and domestication vary in the datasets and approaches, and the types of wild and domesticated breeds compared [23, 28]. Notably, some studies have not included the direct wild ancestors of the domesticated species for comparison. One reason is that the direct wild ancestor of many domesticated species such as horses, dogs, and cattle, are extinct [26, 27]. Directly comparing the recombination landscapes between these domesticated species and the wild populations from which they were not directly derived may introduce bias when assessing the impact of domestication on recombination [23]. As a result, how domestication and continued selection affect the evolution of recombination rates remains controversial.

Chickens have become the most abundant domesticated species, and unlike many

domesticated animals, their direct wild ancestor, the Red Junglefowl (RJF), still exists in South and Southeast Asia. Our earlier study demonstrated that chickens trace their origins to the RJF subspecies *Gallus gallus spadiceus* (GGS). The domestication process, marked by intense and dynamic selection and breeding, led to a significant bottleneck and the accumulation of deleterious mutations [29]. Domestic chickens exhibit lower genetic diversity and a reduction in linkage disequilibrium (LD) over longer distances compared to RJF [29], suggesting alterations in recombination rates and patterns post-domestication. Additionally, as chickens spread globally, they engaged in hybridization with other jungle fowl species, acquiring additional ancestry that likely modified their genetic architecture. Domestic chickens and GGS therefore provide a valuable system to investigate the intricate relationship between domestication and recombination landscapes at finer scales [29, 30].

In this study, we explored recombination rates and profiles in chickens and their wild ancestors by analyzing over 120 whole nuclear genomes of GGS and domesticated chickens, including both village chickens and recently improved commercial breeds. We used a population genomic approach to construct the landscape of recombination for GGS and domestic chicken breeds. We then characterized the variation of recombination at both broad and fine scales, identified recombination hotspots and hotspot motifs, and investigated their genomic features and motifs as well as the associations with recombination, selection, and gene flow. This study offers insights into the landscape of recombination variation in domestication and contributes to our understanding of how domestication and selective breeding affect the evolution of recombination in domesticated species.

RESULTS

The fine-resolution recombination landscape of chicken

We generated whole genome sequences of 17 Red Jungle Fowls of GGS, 20 Jining Bairi Chickens (JNBR), and 20 White Leghorn (WL). The average sequencing depth for each genome is 16.46× (ranging from 7.89× to 26.14×). Additionally, we collected

64 genomes from previous studies, creating a comprehensive dataset of 121 genomes (supplementary Table S1). This dataset encompasses diverse populations, including GGS, four local domesticated chicken (LDC) breeds, namely Chahua (CH), Nixi (NX), JNBR, and Luxi Fighting (LX) chickens, as well as a modern commercial breed WL. Each population is represented by 20 samples. A green jungle fowl (*Gallus varius,* GV) genome was used as an outgroup. After quality control filtering, we identified 7,203,349 (WL) to 14,171,854 (GGS) SNPs per population, corresponding 7.63 to 15.00 SNP per kilobase (kb) (supplementary Table S2). The maximum likelihood tree (supplementary Fig. S1) illustrated distinct clustering of domesticated chickens and GGS into separate groups, with GGS positioned basally to LDC. An exception is WL, which occupies a basal position relative to GGS and LDC, likely due to admixture and carrying high levels of additional ancestry from another divergent RJF lineage, the *G. g. murghi* (GGM) [30]. Compared to GGS, LDC and WL have lower genetic diversity, greater LD decay distance (supplementary Fig. S2, S3), consistent with prior findings that chickens have undergone selective bottlenecks since domestication [29].

We used RelERNN, a deep learning method, to construct a high-resolution recombination rate map from polymorphism data [31]. Both the number of training runs and the sample size could affect the results [31]. To assess the robustness of the results across different parameters, we first tested the effect of the number of training runs by performing 100, 200, 500, 1000, and 2000 simulated training runs. With more than 500 training runs, the correlation coefficient of the predictions exceeded 0.9 (supplementary Fig. S4). Despite additional training (e.g., 1000 and 2000), the correlation only marginally increased, suggesting proximity to saturation. Considering of both consumption of computational resources and accuracy of the results, we conducted 1000 training sessions in subsequent analysis. Then, to explore the effect of sample size on the estimation, we estimated the recombination rate using 5, 10, and 20 samples and found that the estimates showed a high degree of consistency when the sample size was equal to or greater than 10 (Pearson's $r = 0.93$; P value $< 2.2e-16$, supplementary Fig. S5). Hence, 20 samples per population are sufficient to reconstruct their recombination

landscapes. Taken together, these analyses and tests provide a solid justification and foundation for the use of RelERNN to estimate the recombination map.

Considering the differences in genetic background and demography among populations, we estimated the recombination rate for GGS and each of the five domestic chicken populations. We revealed remarkable variations across populations and chromosomes. Among the six populations, the genome-wide average recombination rate was estimated to be 8.85e-10 c/bp, ranging from 3.67e-10 c/bp (WL) to 11.40e-10 c/bp (GGS). Our estimate was in the same order of magnitude as previous estimates in chickens and other birds [32, 33], reinforcing the notion that the genome-wide average recombination rate in chickens is higher than in mammals [34, 35].

The distribution and pattern of recombination rate

One of the striking characteristics of the avian genome is the distinguished length differences between chromosomes, which is also reflected in many genomic features, e.g. GC content, genetic diversity, gene density, as well as recombination rate [32, 36]. We observed a trend emerges with microchromosomes displaying a higher recombination rate than macrochromosomes (mean 7.7e-10 c/bp for macrochromosomes and 10.98e-10 c/bp for microchromosomes). The average Pearson's correlation coefficient for recombination rate (c/bp) versus chromosome length (in Mb) is -0.52 (P value < 0.01; supplementary Fig. S6). We compared the level of recombination with respect to different genomic features, suggesting a positive association between recombination rate and GC content, genetic diversity, and gene density (supplementary Fig. S7). Moreover, compared to introns and intergenic regions, exons exhibit a higher recombination rate, with the promoter regions particularly displaying elevated rates compared to other regions (supplementary Fig. S8). This result is in line with previous studies in other birds [17], monkeyflower [37] and tomato [38], and supports the notion that recombination has been primarily localized to the promoter regions of genes in birds and is also remained highly conserved over millions of years [17].

Prior studies propose a "U"-shaped distribution of recombination rates across the chromosomes in mammalian species, such as mice and humans, with recombination rate tending to be increased near telomeric regions and suppressed in centromeric regions [39-41]. However, in chickens, we did not find an apparent increase in the recombination rate towards distal positions for each autosome. Instead, the distribution of recombination rate exhibited high variation between chromosomes (Fig. 1A). For example, the recombination rate across chromosome 1 displayed a relatively uniform distribution, without a clear central region of decrease and an increase in the distal regions. This result is slightly inconsistent with previous study [32], but aligns more closely with a recent study [42], likely due to the later study employing a larger set of genetic markers and a more complete reference genome. The improvement in the reference genome is likely due to the improved assembly of microchromosomes and subtelomeric regions in most reference genomes, which are notoriously challenging to assemble in birds [43]. Meanwhile, some chromosomes (e.g., chr6, chr8) showed a central region of reduced recombination and an increase in the distal regions, akin to observations in humans and mice [40, 44, 45].

On a broader scale, macrochromosomes and microchromosomes exhibited high difference in recombination landscapes. Microchromosomes displayed significant variability in the distribution of the recombination rate. Some (e.g., chr17, chr18, chr23) exhibited a unimodal distribution of the recombination rate, with peaking in the central regions and a progressive decline towards the ends. On others (e.g., chr21, chr22), recombination decreased at one end but progressively increased towards the opposite end. Additionally, certain chromosomes exhibited a central region of reduced recombination, alongside reductions in subtelomeric regions. This was a prevalent (though not exclusive) pattern in medium-sized chromosomes (e.g., chr15, chr20). However, this may not necessarily indicate a distinct recombination pattern at the telomeres of each chicken chromosome, due to incomplete assembly [43]. Nevertheless, a similar pattern is evident in the previous version of chicken recombination map [32] and other species such as butterflies [1].

Finally, we employed the Gini coefficient to quantitatively measure the degree of inequality in the distribution of the recombination rate [44]. A Gini coefficient value of 0 signifies a uniform distribution, while a coefficient of 1 indicates that all recombination events occur at a single locus. The Gini coefficients for chicken recombination maps range from 0.28 for GGS to 0.40 for WL (supplementary Fig. S9), notably lower than those observed in humans (ranging from 0.688 to 0.771) and mice (ranging from 0.79 to 0.95) [39, 44]. However, it is important to note that Gini coefficients are associated with population size [46], and uncertainties persist regarding whether this pattern reflects the consequences of variations in effective population size between populations [47]. Nevertheless, this result supports the above finding that, compared to mammals, recombination events in chickens are less concentrated in a very restricted subset of chromosomes.

Domesticated chickens displayed a reduced recombination rate

To compare the broad scale recombination map between different populations, we first binned the genomes with 1Mb windows and calculated the Pearson's correlation coefficient (r) for the recombination rate from each pair of populations (supplementary Fig. S10). The Pearson's correlation coefficient ranges from 0.45 to 0.87, suggesting relative conservation of recombination on the broad scale. The phylogenetic relationships of these populations could be accurately reconstructed by the recombination rate, while not nucleotide diversity (supplementary Fig. S11). This supports the prior finding that local mutation rate might be less stable than the fine-scale recombination rate [40].

Microchromosomes display a higher correlation than macrochromosomes (Fig. 1B), aligning with greater conservation of microchromosomes over macrochromosomes in avian species [48]. The populations within LDC show a higher pairwise correlation (Pearson's $r \geq 0.8$) than the WL population. Of particular note, WL display the lowest correlation coefficient of recombination rate compared to domestic chicken breeds and GGS (supplementary Fig. S10), aligning with the result that WL has

the lowest genetic diversity and largest LD decay over distance (supplementary Fig. S2, Fig. S3). These findings underscore the significant impact of recent breeding and selective bottlenecks in shaping the genetic architecture landscape of WL.

Furthermore, among each population, WL display the lowest recombination rate while GGS exhibited the highest (Fig. 2A). To measure the localized changes in recombination rate across the genome, we calculated the ΔRR, the difference in recombination rates between LDC and GGS, using 50-kb sliding windows (Fig. 2B). Within the LDC, 72.79% of regions exhibit a lower recombination rate compared to GGS (ΔRR<0). In WL, a substantial 90.49% of regions display an even lower recombination rate compared to the LDC. To validate this pattern further, we reanalyzed the genomes and estimated the recombination rate for another two chicken breeds (supplementary Table S1), the Beijing YOU chicken (n=10) and Silkie (n=11). They also exhibit a lower genome-wide average recombination rate compared with GGS. In detail, 67.65% and 75.05% of Silkie and Beijing YOU chicken genomes display a lower recombination rate (ΔRR<0), respectively.

To explore if a comparable trend exists in other domestic species, we assessed the recombination rates by re-analyzing the genomes of domestic ducks, goats, pigs, and sheep, along with their respective wild counterparts. Across each species, three domesticated populations were included in this study (supplementary Table S3). Our findings suggest that all domestic breeds exhibited a lower recombination rate compared with their wild relatives (Fig. 2C-F), echoing the observed pattern in chicken populations (Fig. 2A).

While the genome-wide average recombination rate is generally lower in domesticated species than in their wild ancestors, our investigation raises the possibility that intensive artificial selection and breeding may have led to an increased recombination rate in specific genomic regions associated with selected phenotypes and traits. However, our analysis, comparing the association between recombination rate and selection score within putatively selective regions, reveals a negative correlation between local recombination rate and the nSL score (a proxy for the strength of

selection) (supplementary Fig. S12). These observations contradict the notion that domestication and intense selection result in an increased recombination rate in domestic breeds. Instead, our study suggests that domestication likely leads to a decrease in the recombination rate within populations and breeds, not only genome-wide at a broad scale, but also within selective sweep regions.

Characterize recombination hotspots and coldspots

Recombination hotspots exhibit a diverse distribution in eukaryotic organisms that have *PRDM9* [17]. To investigate how selection influences the evolution of recombination hotspots in chickens, we used a previously described method [1] to identify recombination hotspots in each chicken breed using a 1000bp window size. Despite the absence of functional *PRDM9*, we find that chickens yet nonetheless retain recombination hotspots. We identified a total of 265,220 hotspots across all six breeds, with an average of 44,203 per population (Fig. 3A-B), which are distributed non-uniformly across the chicken genome. Although differing in approaches, the number of hotspots in chickens is comparable to estimates for mammals, for example, 25,000-50,000 have been reported in human populations [49].

We performed gene ontology (GO) analysis on genes overlapping with hotspots and coldspots regions. A limited number of statistically enriched GO terms were observed. Notably, genes within recombination hotspot regions are enriched in terms related to immunity, including substance P receptor activity (supplementary Table S4). This finding aligns with studies in other species such as horses, which suggest that recombination occurs more frequently in genes functionally associated with immunity. This association is thought to facilitate robust response, selection and adaptive evolution to changing environments and diseases [50, 51]. Conversely, genes overlapping with the recombination coldspot regions were enriched for terms related to fundamental biological functions such as protein-arginine deiminase activity (supplementary Table S5), echoing observations in butterflies [1]. This suggests a selection against recombination in highly conserved genes and regions [51].

Prior examination of mammals, including humans and mice, demonstrated a considerable influence of the functional genomic elements on local recombination rates [15, 40]. In our study, we reanalyzed ChIP-seq data for 4 histone marks including H3K4me3, H3K4me1, H3K27ac, and H3K27me3 reported in our previous study [52] and measured the recombination rate for these histone-marked regions. Our findings reveal variations in recombination rates among different chromatin states. Regions associated with H3K4me3, H3K4me1, H3K27me3 and H3K27ac showed significantly higher recombination rates than expected by randomly selected regions in chickens (P value < 0.001, n=1000 times; Fig. 3C). Our result suggests that the recombination event usually accompany the histone chromatin modifications, consistent with prior research indicating that double-strand breaks (DSBs) tend to occur in regions proximal to histone modifications in *PRDM9* knockout mice [15]. Although a causal relationship has yet to be established, this suggests that these histone modifications are also necessary to create a favorable chromatin environment for the initiation of meiotic recombination in birds. It is noteworthy that both recombination rates and chromatin structure are susceptible to temporal changes. Our recombination estimates offer a historical average for each population, whereas chromatin state modifications are derived from contemporary samples. This inconsistency may potentially introduce limitations to the analysis, despite the prior comparison between them.

Recombination hotspots and coldspots evolve rapidly in the chicken populations

We compared the number of shared hotspots among chicken populations and observed remarkable variation (Fig. 3A). Thousands of hotspots were unique to specific populations, with only 3 hotspots shared by all domestic populations. Domestic populations, with the exception of WL, shared more hotspots with domestic populations than with GGS. WL, on the other hand, shared the fewest hotspots with others, suggesting recent breeding has resulted in rapid hotspot variation. Furthermore, we examined the frequency of recombination hotspots and coldspots overlapping with selective sweeps. The overlap between the recombination hotspots and selective sweeps

was approximately 3.86%, which is less than expected by chance when compared to the randomly selected regions (approximately 8.09 ± 0.9%, one-sample t-test, P value < 0.001), suggesting that most of the selective sweeps occur outside the hotspot. In contrast, the overlap between coldspot and the selective sweeps (approximately 19.44%) exceeds the expected value compared to the randomly selected regions (approximately 5.66 ± 0.7%; one-sample t-test, P value < 0.001). It is important to note that although empirical approaches are commonly used to find the signal of sweep regions, they may introduce bias and cannot rule out false positives. To further explore our analysis, we systematically retrieved putatively selective sweeps with progressively more relaxed empirical cut-offs (from the top 1% to 5% and 10%), expecting an increase in false positives. Consistent with our expectation, the proportion of overlap between coldspot and putatively selective sweeps progressively decreases (from 19.44% to 9.47% and 6.64%), and the frequency between hotspot and selective sweeps is progressively increases (from 3.86% to 4.71% and 7.01%; supplementary Fig. S13), which also suggesting that selective sweeps favor regions of low recombination.

A previous study on tomato demonstrated that the majority of selective sweeps were outside the recombination hotspot [53], consistent with our findings. In great apes, the majority of the recombination coldspots also largely overlapped with selective sweeps [54]. Therefore, domestication likely leads to the loss of the hotspot and/or the emergence of the coldspot, highlighting a specific way in which domestication results in a decreased recombination rate [53].

Identify the recombination hotspot determinants by deep learning method

In humans, the DNA-binding protein PRDM9 is the factor that controls the localization of recombination hotspots by specifically binding to the 13-bp consensus DNA motif: CCNCCNTNNCCNC [49]. To examine whether chickens lacking functional *PRDM9,* possess DNA-binding motifs and sequences associated with hotspots, we leveraged RHSNet [55] to predict the potential determinant motifs of recombination hotspots in each chicken population (Fig. 4A). Across all six chicken

populations, the GC content of the top 100 predicted motifs is significantly higher than that of the entire genome (62.02% vs. 45.43%; Fig. 4C). This is in line with previous studies that the recombination hotspot often occurs at CpG islands (CGIs), and genomic regions with elevated GC content. To provide a detailed representation of the motif embeddings, we followed a previous study [55] and visualized the motifs in 2-mer occurrence frequency (Fig. 4A). The occurrence frequency of the 2-mer motif exhibits a high correlation among each population (Pearson's $r \geq 0.8$; Fig. 4B). The 2-mer motif in WL exhibited a higher correlation with other populations (average Pearson's $r = 0.90$) compared to the correlation of broad-scale recombination between WL and others (average Pearson's $r = 0.47$). Notably, the $\{GG\}_n$ motif exhibits extremely high enrichment and had a high frequency in each population. This finding is consistent with the observations in human populations [55], which collectively suggest that although the location of the hotspot shows high variation, the binding motif for the recombination determinant remains relatively conserved in recently diverged populations.

The correlation between recombination rate and introgressed ancestry

Hybridization with closely related wild species commonly occurs in domesticated species as they expand from their origin center [56]. These introgressed materials often facilitate the adaptive evolution of domesticated species [57, 58]. The recombination rate plays a crucial role in determining the pattern and frequency of introgressed ancestry [59]. Positive correlations between the rate of recombination and the level of introgressed ancestry have been observed in many organisms, such as swordtail fish [60], house mice [61] and butterflies [62], attributed to the purging of deleterious mutations within introgressed regions because of incompleteness. To investigate the relationship between the amount of introgression and recombination rate in chickens, we focus on WL, a commercial breed that hybridized with GGM (diverged from chickens ~80 kya) and then inherited over 10% of its genetic ancestry from GGM [30]. Strikingly, we identified a weak negative correlation between the frequency of introgressed ancestry and the rate of recombination (Fig. 5, supplementary Fig. S14),

regardless of whether Loter [63], fd [62] or FLARE [64] was used to identify GGM introgressed ancestry.

We further examined the overlap proportions between introgressed regions and recombination coldspots/hotspots. The overlap between coldspots and introgressed regions, is significantly higher than expected by chance from randomly selected regions (21.62% vs. 5.57%; permutation test, P value < 0.001). In contrast, the overlap between recombination hotspots and introgressed regions is significantly lower than expected by chance from randomly selected regions (0.78% vs. 7.97%; permutation test, P value < 0.001). Interestingly, when a statistically stricter cut-off was used to retrieve the introgressed regions, a lower proportion of overlap was found between hotspots and these introgressed regions (supplementary Fig. S15). This result aligns with our previous finding that introgressed ancestry in WL is more likely to be obscured at regions of low recombination, contrary to empirical investigations of hybridization and recombination rates in the majority of species.

Demography, such as population expansion and contraction, could influence recombination patterns and genetic dynamics [59, 65, 66]. As a commercial breed, WL has experienced continuous selection bottlenecks and maintained a long-term small population size [29]. We speculate that the long-term small population size of WL may be a factor contributing to the unexpected negative correlation between recombination rate and introgression level. To test this, we performed a simulation analysis. Our models considered the demographic history of chickens and RJFs [29, 30] and simulated the scenarios with four populations having a topology (((P1, P2), P3), O) reflecting the phylogeny and splitting of GV, GGM, GGS, and WL (Fig. 5C) where the P3 (donor), with a splitting of 80 thousand years from P1 and P2, contributed 10% of the gene flow to the recipient population (P1). We assumed various population sizes for the recipient population in different models and measured the overlapping frequency of gene flow and recombination rate. When the effective population size for the recipient population was larger (e.g., 2 times and 10 times) than the donor population, the frequency of gene flow was positively correlated with the level of recombination rates

in scenarios where (Fig. 5D; supplementary Fig. S16). However, in scenarios where the recipient population size is reduced to 10% and 20% of the donor population size, the frequency of introgressed ancestries is negatively correlated with the level of recombination rates. These analyses suggest that the population size of the recipient population influences the correlation between the frequency of gene flow and the recombination rate. Thus, prolonged small population size of WL resulting from selective breeding may be the potential factor leading to the negative correlation between recombination rate and introgression frequency.

DISSCUSSION

Recombination rate is decreased in domesticated species

In this study, we used population genomic approaches to construct the recombination maps for both local and commercial chickens alongside their wild relatives. Our maps greatly improve the resolution compared to a prior version based on a limited dataset from mapping populations [32], thereby providing a valuable opportunity for comparative studies. We have shown that, although chickens lack the recombination-determining gene *PRDM9*, the landscape of recombination rate and profile is rapidly evolving between chicken breeds. Both modern commercial breeds and local chicken populations exhibit remarkably lower recombination rates than their wild relatives. And the similar patterns were reproduced in ducks, goats, pigs, and sheep. These findings collectively suggest that a decreased effective broad-scale recombination in domestic populations is a common occurrence in the process of species domestication, refusing the hypothesis of Rees and Dale (1974) that recombination is increased in domestic populations [67]. However, our findings support the prediction by Lenormand and colleagues that a reduced recombination rate in domesticated species may protect against maladaptive gene flow from wild relatives [25]. This may be true, because, as domestic chickens spread across the continent soon after they were domesticated in northern Southeast Asia, they hybridized with and acquired additional genetic alleles from wild RJF subspecies and other junglefowl

species, which had divergent from domestic chickens over tens of thousands to millions of years [30]. This observation is supported by empirical evidence indicating a decline in recombination rate during post-domestication across various species such as maize [68], tomato [53], and some domestic animals including dogs, goats and sheep [26], with maize demonstrating an 82.3% reduction compared to wild progenitors.

Selective breeding in both domestic animals and crops commonly aims for phenotypic uniformity, as evident in various studies [69, 70]. This practice involves rigorous selection to eliminate non-uniform traits and promote consistency. A reduced rate of recombination plays a pivotal role in preserving haplotypes, which in turn fosters consistency in phenotypes. Consequently, we hypothesize that a decreased recombination frequency would be advantageous in maintaining uniformity and stability of phenotypic traits within domestic breeds during selective breeding processes. Therefore, it is plausible that a diminishing rate of recombination is likely to be consciously or unconsciously favored and selected for in domesticated species to mitigate phenotypic uniformity and address incompatibilities arising from introgressed ancestry.

Recombination hotspot evolves rapidly through domestication

We demonstrated a certain degree of correlation in the broad scale of recombination between chicken breeds and their wild relatives, yet there was a significant order of magnitude variation in the number and location of hotspots. Notably, many hotspots are unique to specific populations, highlighting a considerable variation in hotspot usage within chickens. It is important to acknowledge that our hotspot and coldspot identification method is purely computational, lacking experimental validations, which could potentially lead to false positives. Specifically, we identified more hotspots in domestic chickens compared to GGS. However, this doesn't necessarily imply that all of these hotspot regions in chickens emerged recently and exhibited increased recombination rates during domestication. Instead, it is also likely a reflection of decreased recombination near the surrounding regions and the rest of the

backgrounds in domestic chickens. Nevertheless, our findings align with observations in other recently diverged three-spined sticklebacks that recombination landscapes are highly divergent, with only approximately 15% of hotspots shared between different species [71]. In rice, about 80% of hotspots were unique to each subspecies [71]. In chimpanzees and humans [72, 73], horse breeds [51] , mouse strains [44], and tomatoes [53], rapid turnover of hotspots has also been reported. Therefore, hotspots are likely to be short-lived and rapidly evolving, which may vary depending on selection pressure, demographic history and genomic background [74]. Rapid turnover of the hotspot may be a mechanism shaping the recombination evolution, which is probably associated with speciation, adaptation and selective advantage.

Our study reveals notable similarities in the evolutionary patterns among the chicken and mammals, despite they diverged over hundreds of millions of years. For example, the broad-scale recombination rate remains consistent among chicken populations, while the number and occurrence of hotspots vary, aligning with observations in mouse strains [74], horses [51] and human populations [44]. A previous study showed that the determinants governing the location and behavior of individual hotspots operate independently of regulatory systems controlling regional recombination rates [2]. The presence of large breed-specific hotspots in chicken populations suggests that intense artificial selection during domestication may favor these regulators, although the nature of these factors in birds remains unknown.

Recombination rate is negatively correlated with the frequency of introgressed ancestry

Recombination is a primary determinant of gene flow, and a positive correlation between recombination rate and introgressed ancestry has usually been reported, which is thought to prevent deleterious mutations from gene flow due to incompatibilities. However, we observed an unusual pattern wherein the recombination rate in WL exhibited a negative correlation with the frequency of introgressed ancestry from GGM (Fig 5A-B; supplementary Fig. S14). Our simulation analysis indicated that an

extremely small population size of the recipient WL population, resulting from long-term selective bottleneck compared to donor population could explain this phenomenon. GGM and WL have undergone substantial divergence, facing unique selection pressures and demographic change, suggesting the potential evolution of genomic compatibilities between them. Selection eliminates hybrid ancestry, particularly in regions characterized by low recombination and functional significance, thereby likely leading to a negative correlation between the recombination rate and the frequency of introgressed ancestry [75]. Our study, echoing the conclusions of a pr investigation and contributing a case to support their population simulation analysis, which indicates that admixture between populations can lead to a temporary reduction of genetic load in smaller recipient populations, resulting in an increased frequency of introgressed ancestry, especially when recombination rates are low [59].

A previous study of North American of *D. melanogaster* populations also found a negative correlation between recombination rate and introgressed ancestry [76]. Our results may present an alternative explanation for this observed pattern. However, it is important to note that changes in population size are not the sole factors contributing to the negative correlation between recombination and introgressed ancestry. Other potential factors in the domestication process, such as selection and adaptive introgression, either individually or in combination, may also influence this pattern. For instance, research on human, pig, and dog genomes has revealed that pervasively adaptive regions can introduce long linkage blocks into regions of low recombination [77-79]. Further investigation is warranted to elucidate the intricate interplay between introgression levels and recombination rates.

CONCLUSIONS

Overall, we have presented a detailed recombination map for both chickens and red jungle fowl, shedding light on the intricacies of recombination variation during the process of domestication. Through a comprehensive re-analysis of the genomes of ducks, goats, pigs, and sheep, along with their wild counterparts, we demonstrate a

consistent reduction in recombination rates as a consequence of domestication, challenging the hypothesis proposed by Rees and Dale in 1974. Our findings highlight significant alterations in both broad and fine-scale recombination patterns due to domestication and inbreeding. Considering the variations in genetic structure, selective pressures, and admixture among domesticated populations, our results, coupled with previous studies, underscore the highly dynamic landscape of recombination, even among populations with recent divergence and under dynamic selection forces. This implies that a singular recombination map may not adequately capture the variations within a species. Looking forward, as genome sequencing costs decrease, the development of population-specific recombination maps holds promise for enhancing population genomic studies. Such maps can also aid in refining the identification and control of the inheritance of preferred genetic haplotypes and causative mutations for specific traits in domesticated species. It is crucial to acknowledge the limitations of our population approach, particularly in estimating recombination crosses using genetic variants and heterozygous. Despite our use of medium to high coverage genomes to mitigate potential biases in variant calling, the extended process of domestication and selective breeding likely results in the loss of genetic variants and increased homozygosity in the genome. We acknowledge the possibility of underestimating true recombination crosses within homozygous tracts. Nevertheless, our study contributes to the growing body of evidence on the evolution of recombination rates within and between populations undergoing domestication and selection. This knowledge has implications for population genomics and breeding practices, offering insights that can shape future research and applications in the field.

MATERIALS AND METHODS

Sampling and genome sequencing

Blood samples were obtained from 57 individuals, comprising 17 from the GGS, 20 from the WL, and 20 from the JNBR, and were stored in a freezer before DNA extraction. The GGS samples were collected earlier from Ruili in Yunnan province of

China, while the WL samples were sourced from the farm of China Agricultural University. The JNBR samples were acquired from Shandong Hundred-Day Chicken Poultry Breeding Co., Ltd. DNA extraction was carried out using the phenol-chloroform extraction method. Paired-end DNA sequencing libraries were prepared, and sequencing was conducted on the Illumina NovaSeq 6000 platform, generating a total of 350.74 gigabytes of raw data. Detailed information regarding the sequencing data is available in supplementary Table S1. Additionally, genome re-sequencing data for 105 individuals from four domestic breeds, including 20 LX, 20 NX, 20 CH, 10 YOU, 11 SK, 20 GGM, 3 GGS along with a green junglefowl (*Gallus varius*; GV) genome used as an outgroup, were retrieved from the NCBI SRA database and ChikenSD (http://bigd.big.ac.cn/chickensd/; details could be found in supplementary Table S1).

Sequencing alignment and variant calling

We removed the low-quality bases and reads using the trimmomatic v0.39 tool [80] with parameters: "PE -threads 10 LEADING:3 TRAILING:3 SLIDINGWINDOW:4:15 MINLEN:36". After qualification, all cleaned data were mapped to the chicken reference genome (GRCg7b) using default parameters except "-t 8 -M" option. We conducted processing on the BAM alignment, including coordinate sorting, marking duplicated reads, local realignment, and recalibrating base quality scores, utilizing the Picard (version 3.1.1; https://broadinstitute.github.io/picard/) and GATK (version 4.0; https://gatk.broadinstitute.org/hc/en-us) packages [81]. The average depth of coverage and the mapping ratio were provided in supplementary Table S1. We called SNPs following the GATK best practices pipeline [81] using tools HaplotypeCaller and GenotypeGVCFs. We filtered out low-quality variants using the following criteria: "QD < 2.0 || FS > 60.0 || MQ < 40.0 || SOR > 3.0 || MQRankSum < -12.5 || ReadPosRankSum < -8.0". As a result, 32,882,582 SNPs were obtained after quality filtration. To ensure the robustness of the dataset for each population, variants

with minor allele frequencies below 0.05 and missing genotypes exceeding 20% in each population were meticulously excluded.

To further examine our result, we expanded our analysis to include whole-genome genotyping of ducks, pigs, yaks, and sheep. Genotyping data for these species were sourced from previous studies (supplementary Table S3). Within each of these four species, there are four distinct breeds, each consisting of about 10 individuals.

Population structure and phylogeny analysis

We meticulously examined the population structure across the entire genome for both GGS and domestic chicken breeds. We actively filtered SNPs based on linkage disequilibrium (LD) pruning using PLINK v1.9 [82], employing the arguments: "-indep-pairwise 50 5 0.2". Importantly, we deliberately excluded the sex chromosomes from our analysis. Leveraging this data, we constructed a maximum likelihood tree using the iqtree tool [83], with parameters “-m TEST -st DNA -bb 1000 -nt AUTO”. Subsequently, we calculated the population LD decay using LDpopdecay [84] and visually presented the LD decay profiles for all groups with default parameters.

Genomic summary statistics and selective sweep analysis

We performed a comprehensive analysis of genetic features within the genome of each breed and explored their correlation with recombination rate by calculating various summary statistics. For an in-depth examination of gene density and GC content across the chicken genome, we evaluated the proportion of gene regions in 2 Mb non-overlapping sliding windows based on the gene model annotation file (gff format). To determine the genetic diversity within the six chicken breeds, we calculated the nucleotide diversity (pi) for each breed using vcftools with the parameters "--window-pi 50000" [85].

We used selscan version 1.3.0 [86] to identify genomic regions with signals of selection in each breed. Genome-wide nSL scores were normalized with selscan’s companion program norm from selscan using default parameters. We partitioned the

genome into non-overlapping 50-kb regions and calculated the fraction of sites with |nSL| > 2 in each window. We then selected the windows with the top 1%, 5%, and 10% of the fraction of sites with high scores as potential sweeps, which were used for further detailed analysis.

Inference of locally introgressed ancestries

Using high-quality sequencing datasets comprising 20 samples from WL, 20 from CH, and 20 from GGM (supplementary Table S1), we identified segments in the WL population that were introgressed by GGM. First, we calculated "fd" [62, 87], a metric based on the calculation of ABBA-BABA sites in the four-taxon topology (((P1, P2), P3), O), to detect and quantify bidirectional introgression at specific loci. In our calculation, we designated the CH, WL, and GGM populations as P1, P2, and P3, respectively, with a green junglefowl serving as the outgroup. We calculated "fd" values using a 100 kb sliding window with 20 kb increments, utilizing the command: "ABBABABAwindows.py -w 100000 -m 10 -s 20000 ChrN.vcf.geno.gz -o fd.csv.gz -f phased --minData 0.5 --writeFailedWindow -P1 CH -P2 WL -P3 GGM -O GV --popsFile pop.info". Windows with fdM>0 and the number of informative sites ≥ 10 were retained as outlier loci. Second, we constructed FLARE [64], the most recent method for estimating leaf area index (LAI). It was a site-based generative method derived from HapMix [88], and exhibits commendable efficiency and accuracy due to its tailored optimization for computational resources and the flexibility of its model, which allows for adjustable parameters to accommodate different scenarios. For our study, we chose CH and GGM as reference panels, with WL representing the mixed population. We then performed calculations to determine the length and frequency of ancestral segments within each reference group in WL using the command "java -jar flare.jar ref=CH_GGM_ChrN.vcf ref-panel=CH_GGM.list.txt min-mac=20 gt=WL_ChrN.vcf map=CH_GGM_ChrN.map.txt out=WL_CH_GGM_ChrN_flare".

Finally, we utilized Loter to infer local ancestry, a method demonstrated to be robust in detecting more ancient admixtures, to obtain admixed ancestry in WL from

GGM [63]. We specified the GGM and CH as reference panels, with WL being the admixed population with the command "loter_cli -a WL.ChrN.vcf -r ChaHua.ChrN.vcf GGM.ChrN.vcf -f vcf -n 6 -v -pc -o WL.ChrN.CH-GGM.Loter.txt". Loter determines the most likely ancestral origin for each fragment using allele frequencies from the reference and selected populations. Introgression percentages from GGM into haploid genomes were calculated, and overlapping introgressed regions from the same source were merged. Frequencies were then calculated for each selected fragment across the WL.

Recombination rate estimation

We used RelERNN (v1.0.0) to estimate population-scale recombination rates for each chromosome in six chicken populations [31]. RelERNN uses recurrent neural networks, and takes columns from a genotype alignment, which are then modelled as a sequence across the genome using a recurrent neural network. We simulated and trained the datasets with parameters based on the developers' recommendations [42].

To evaluate the robustness of our results across different parameters, we examined the impact of different gradient parameters and identified the "--nEpochs" parameter as the most influential. Consequently, we performed several simulated training runs, varying the "--nEpochs" parameter from 100 to 2000 iterations (100, 200, 500, 1000, and 2000). Remarkably, using more than 500 training runs (--nEpochs 500) resulted in a correlation coefficient greater than 0.9. Despite additional training efforts (e.g., 1000 and 2000 runs), the correlation showed only marginal improvement, suggesting near saturation. Considering the computational resources used, we chose 1000 training runs for the subsequent analyses.

To explore the effect of sample size on the estimation accuracy, we used RelERNN to estimate the recombination rate using 5, 10, and 20 samples with the settings "--nEpochs 1000, MU=1.91e-9, --nTrain 100000, --nVali 1000, --nTest 1000, and --nValSteps 20". We measured the correlation of each estimate using Spearman's

correlation. Notably, our results showed a high degree of consistency in the estimates when the sample size was 10 or greater.

Therefore, based on the results of the above tests, we estimated recombination rates for GGS and each chicken breed, as well as combining all samples (including both GGS and domestic chickens) using parameters "--nEpochs 1000, MU=1.91e-9, --nTrain 100000, --nVali 1000, --nTest 1000, and --nValSteps 20" with 20 samples per chicken breed. We then standardized them into non-overlapping 50-kb windows. Sex chromosomes and dot chromosomes (Chr16, 29-32,34 and 39) were excluded from the analyses because of incomplete assembly and the large proportion of missing rate.

The similarity of recombination distribution among chicken breeds was assessed using Pearson's correlation, both for whole genome comparisons (1 Mb intervals) and individual chromosomes. The genomic distribution of recombination rates in each population was summarized using the Gini coefficient [89]. The Review of Economics and Statistics Gini coefficients describe inequality by summarizing the dispersion of a quantitative measure, which is a popular measure for summarizing inequality [90].

Identify recombination hotspots and coldspots

Recombination hotspots and coldspots were identified according to methods outlined in a prior study [1]. First, we divided the recombination map into non-overlapping 1kb windows. Hotspots were characterized as regions exhibiting a recombination rate at least 2 times higher than the regional "background" rate, determined as the average rate for the focal window and its two flanking windows. Conversely, coldspots were regions with a recombination rate at least 10 times lower than the regional background rate.

To evaluate overlap with selective sweeps, gene flow, etc., and assess chance outcomes, we generated 100/10,000 sets of random, size-matched genomic segments to mimic detected hotspots/coldspots using "shuf -n". These simulated regions were termed "randomspots," and overlap was assessed using bedtools intersect. Fisher’s

Exact tests identified genomic features with differential enrichment between hotspots/coldspots.

Hotspots were further analyzed for proximity to promoters, coding sequences (CDS), and intergenic regions. Overlap with previously published double-strand break (DSB) hotspots identified by ChIP-seq was also examined using the intersect function in the bedtools software following the previous study [91]. Additionally, we analyzed hotspot/coldspot overlap within and between subspecies by examining population-specific sets using bedtools intersect.

The investigation focused on the analysis of Gene Ontology (GO) terms associated with genes located within hotspots and coldspots identified by all the eight chicken breeds. To conduct this analysis, gene data, including GeneIDs, was obtained from Ensembl via Biomart. The subsequent analysis involved the application of bedtools to assess the overlap of GO terms. The genes were further categorized based on their involvement in biological processes (GO_BP), cellular components (GO_CC), and molecular functions (GO_MF). This classification was achieved using g:Profiler [92] with a criterion of P-value < 0.1 corrected by the Benjamini & Hochberg method.

Identify recombination hotspot determining motif

To determine whether there are any critical motifs involved in chicken recombination hotspots, we employed RHSNet, a cutting-edge tool rooted in deep learning and signal processing [55]. RHSNet is tailored to predict significant motifs contributing to recombination hotspots specifically in chickens. Our methodology commenced with constructing a comprehensive dataset for 5-fold cross-validation and motif extraction, incorporating datasets such as the Icelandic Human dataset [93], the HapMap II dataset [94], the Sperm dataset [95], hotspots and coldspots derived from paternal and maternal maps of the Icelandic Human dataset [93], along with the mouse dataset [96]. Then, we conducted training sessions, including Baseline CNN training, Equivalent CNN training, RHSNet training, RHSNet-Chip training with consideration for sexual differences, and Baseline CNN training on the 1000 Genome Dataset. For

motif extraction, we employed the Python script "motif_extractor.py" from RHSNet, facilitating the identification and analysis of key motifs within the chicken recombination hotspots.

Simulation analysis

To explore the impact of effective population size on the correlation between recombination and gene flow, we conducted the simulation analysis. Our model is grounded in a four-population topology (((P1, P2), P3), O) reflecting the phylogeny and splitting of GV, GGM, GGS, and WL. In the model, P4 diverged from P1-P2-P3 around 4 million years ago, P3 diverged from P1-P2 approximately 80,000 years ago [29, 30], and P1 diverged from P2 around 10,000 years ago, and divergent P3 population (donor) contributed 10% of the gene flow to the recipient P1 population. P3 and P2 maintain a consistent population size of N0, while P1 exhibits different population sizes in various models. We tested five models in which P1 has population sizes of 10*N0, 2*N0, N0, 0.2*N0, and 0.1*N0, respectively, in 200 years (corresponding to the breeding history of WL). In each model, we used msprime [97] to simulate 2, 40, 40, and 40 haplotypes with a length of 2Mb for O, P3, P2, and P1, respectively. Thirty replicates were performed for each simulation. Utilizing the simulated data, we used Loter to identify P3 introgressed segments in P1, and estimated the recombination rates using RelERNN. Subsequently, we measured the Pearson's correlation between the frequency of introgressed ancestry and recombination rate. In our simulations, N0 was set to 10000, and the mutation rate (per site per year) was set to 1.91e-9.

CONFLICT OF INTEREST

The authors declare that they have no conflict interest.

ACKNOWLEDGMENTS

This work was supported by the National Key Research and Development Program of China (2023YFF1001000) and the Yunnan Fundamental Research Projects

(202301AW070012, 202401AV070007), Yunnan Province (202305AH340006) and the "Yunnan Revitalization Talent Support Program: High-end Foreign Expert Project and Young Talent Project (XDYC-QNRC-2022-0770)". The National Natural Science Foundation of China, Talent Program of Chinese Academy of Sciences (CAS) and Animal Branch of the Germplasm Bank of Wild Species of CAS (the Large Research Infrastructure Funding) also supported this project. A.E. was supported by the CAS President's International Fellowship Initiative (No. 2024VBA0001). We would like to thank Hong-Man Chen for his help in drawing the figures.

AUTHOR CONTRIBUTIONS

Ming-Shan Wang, Ya-Ping Zhang, and Jian-Lin Han conceived the project and designed the research. Zheng-Xi Liu and Ming-Shan Wang performed the analysis. Jian-Lin Han and Lu-Jiang Qu collected samples and prepared the DNA samples and contributed genome sequencing data. Ming-Shan Wang and Zheng-Xi Liu drafted the manuscript with input from all authors. Ming-Shan Wang, Ming Li, Ya-Ping Zhang, Si Si, Jian-Lin Han, Jian-Hai Chen, Chang Zhang, Li-Rong Hu, Min-Sheng Peng, Ting-Ting Yin, Ali Esmailizadeh, and Xue-Mei Lu revised the manuscript. All authors read and improved the final manuscript.

DATA AVAILABILITY

The 57 whole genomes we generated were submitted to GSA (https://ngdc.cncb.ac.cn/gsa/) under the accession number PRJCA025697. Scripts and recombination estimations are available at https://github.com/Joyce121.

SUPPLEMENTARY DATA

Supplementary tables and figures are available at Supplementary information.

REFERENCES

1. Palahi ITA, Hook L, Nasvall K *et al.* The fine-scale recombination rate variation and associations with genomic features in a butterfly. *Genome Res* 2023; **33**(5): 810-823.
2. Paigen K, Petkov P. Mammalian recombination hot spots: properties, control and evolution. *Nat Rev Genet* 2010; **11**(3): 221-233.
3. Fransz P, Linc G, Lee CR *et al.* Molecular, genetic and evolutionary analysis of a paracentric

inversion in Arabidopsis thaliana. *Plant J* 2016; **88**(2): 159-178.
4. Marand AP, Zhao HN, Zhang WL *et al.* Historical Meiotic Crossover Hotspots Fueled Patterns of Evolutionary Divergence in Rice. *Plant Cell* 2019; **31**(3): 645-662.
5. Dutta R, Mainsah J, Yatskiv Y *et al.* Intricacies in arrangement of SNP haplotypes suggest "Great Admixture" that created modern humans. *Bmc Genomics* 2017; **18**(1):433.
6. Battagin M, Gorjanc G, Faux AM *et al.* Effect of manipulating recombination rates on response to selection in livestock breeding programs. *Genet Sel Evol* 2016; **48**(1): 44.
7. Epstein R, Sajai N, Zelkowski M *et al.* Exploring impact of recombination landscapes on breeding outcomes. *Proc Natl Acad Sci U S A* 2023; **120**(14): e2205785119.
8. Stapley J, Feulner PGD, Johnston SE *et al.* Variation in recombination frequency and distribution across eukaryotes: patterns and processes. *Philos Trans R Soc Lond B Biol Sci* 2017; **372**(1736): 20160455.
9. Dreissig S, Mascher M, Heckmann S. Variation in Recombination Rate Is Shaped by Domestication and Environmental Conditions in Barley. *Mol Biol Evol* 2019; **36**(9): 2029-2039.
10. Hoge C, de Manuel M, Mahgoub M *et al.* Patterns of recombination in snakes reveal a tug-of-war between PRDM9 and promoter-like features. *Science* 2024; **383**(6685): eadj7026.
11. Jones JC, Wallberg A, Christmas MJ *et al.* Extreme Differences in Recombination Rate between the Genomes of a Solitary and a Social Bee. *Mol Biol Evol* 2019; **36**(10): 2277-2291.
12. Penalba JV, Wolf JBW. From molecules to populations: appreciating and estimating recombination rate variation. *Nat Rev Genet* 2020; **21**(8): 476-492.
13. Hochwagen A, Marais GA. Meiosis: a PRDM9 guide to the hotspots of recombination. *Curr Biol* 2010; **20**(6): R271-274.
14. Auton A, Fledel-Alon A, Pfeifer S *et al.* A fine-scale chimpanzee genetic map from population sequencing. *Science* 2012; **336**(6078): 193-198.
15. Brick K, Smagulova F, Khil P *et al.* Genetic recombination is directed away from functional genomic elements in mice. *Nature* 2012; **485**(7400): 642-645.
16. Hinch AG, Tandon A, Patterson N *et al.* The landscape of recombination in African Americans. *Nature* 2011; **476**(7359): 170-175.
17. Singhal S, Leffler EM, Sannareddy K *et al.* Stable recombination hotspots in birds. *Science* 2015; **350**(6263): 928-932.
18. Axelsson E, Webster MT, Ratnakumar A *et al.* Death of PRDM9 coincides with stabilization of the recombination landscape in the dog genome. *Genome Res* 2012; **22**(1): 51-63.
19. Lam I, Keeney S. Nonparadoxical evolutionary stability of the recombination initiation landscape in yeast. *Science* 2015; **350**(6263): 932-937.
20. Singhal S, Leffler EM, Sannareddy K *et al.* Stable recombination hotspots in birds. *Science* 2015; **350**(6263): 928-932.
21. Roze D. A simple expression for the strength of selection on recombination generated by interference among mutations. *Proc Natl Acad Sci U S A* 2021; **118**(19): e2022805118.
22. Otto SP, Barton NH. The evolution of recombination: Removing the limits to natural selection. *Genetics* 1997; **147**(2): 879-906.
23. Ross-Ibarra J. The evolution of recombination under domestication: a test of two hypotheses. *Am Nat* 2004; **163**(1): 105-112.
24. Gornall RJ. Recombination systems and plant domestication. *Biological Journal of the Linnean Society* 1983; **20**(4): 375-383.

25. Lenormand T, Otto SP. The evolution of recombination in a heterogeneous environment. *Genetics* 2000; **156**(1): 423-438.
26. Larson G, Burger J. A population genetics view of animal domestication. *Trends Genet* 2013; **29**(4): 197-205.
27. Larson G, Piperno DR, Allaby RG *et al.* Current perspectives and the future of domestication studies. *Proc Natl Acad Sci U S A* 2014; **111**(17): 6139-6146.
28. Munoz-Fuentes V, Marcet-Ortega M, Alkorta-Aranburu G *et al.* Strong artificial selection in domestic mammals did not result in an increased recombination rate. *Mol Biol Evol* 2015; **32**(2): 510-523.
29. Wang MS, Zhang JJ, Guo X *et al.* Large-scale genomic analysis reveals the genetic cost of chicken domestication. *BMC Biol* 2021; **19**(1): 118.
30. Wang MS, Thakur M, Peng MS *et al.* 863 genomes reveal the origin and domestication of chicken. *Cell Res* 2020; **30**(8): 693-701.
31. Adrion JR, Galloway JG, Kern AD. Predicting the Landscape of Recombination Using Deep Learning. *Mol Biol Evol* 2020; **37**(6): 1790-1808.
32. Groenen MA, Wahlberg P, Foglio M *et al.* A high-density SNP-based linkage map of the chicken genome reveals sequence features correlated with recombination rate. *Genome Res* 2009; **19**(3): 510-519.
33. Provost K, Shue SY, Forcellati M *et al.* The Genomic Landscapes of Desert Birds Form over Multiple Time Scales. *Mol Biol Evol* 2022; **39**(10): msac200.
34. Stapley J, Feulner PGD, Johnston SE *et al.* Variation in recombination frequency and distribution across eukaryotes: patterns and processes. *Philos T R Soc B* 2018; **372**(1736): 20160455.
35. Beeson SK, Mickelson JR, McCue ME. Exploration of fine-scale recombination rate variation in the domestic horse. *Genome Res* 2019; **29**(10): 1744-1752.
36. Fullerton SM, Bernardo Carvalho A, Clark AG. Local rates of recombination are positively correlated with GC content in the human genome. *Mol Biol Evol* 2001; **18**(6): 1139-1142.
37. Hellsten U, Wright KM, Jenkins J *et al.* Fine-scale variation in meiotic recombination in Mimulus inferred from population shotgun sequencing. *Proc Natl Acad Sci U S A* 2013; **110**(48): 19478-19482.
38. de Haas LS, Koopmans R, Lelivelt CLC *et al.* Low-coverage resequencing detects meiotic recombination pattern and features in tomato RILs. *DNA Res* 2017; **24**(6): 549-558.
39. Stevison LS, Woerner AE, Kidd JM *et al.* The Time Scale of Recombination Rate Evolution in Great Apes. *Mol Biol Evol* 2016; **33**(4): 928-945.
40. Spence JP, Song YS. Inference and analysis of population-specific fine-scale recombination maps across 26 diverse human populations. *Sci Adv* 2019; **5**(10): eaaw9206.
41. Nowosad A, Jeannot P, Callot C *et al.* p27 controls Ragulator and mTOR activity in amino acid-deprived cells to regulate the autophagy-lysosomal pathway and coordinate cell cycle and cell growth. *Nat Cell Biol* 2020; **22**(9): 1076-1090.
42. Weng Z, Wolc A, Su H *et al.* Identification of recombination hotspots and quantitative trait loci for recombination rate in layer chickens. *J Anim Sci Biotechnol* 2019; **10**: 20.
43. Li M, Sun C, Xu N *et al.* De Novo Assembly of 20 Chicken Genomes Reveals the Undetectable Phenomenon for Thousands of Core Genes on Microchromosomes and Subtelomeric Regions. *Mol Biol Evol* 2022; **39**(4): msac066.
44. Wooldridge LK, Dumont BL. Rapid Evolution of the Fine-scale Recombination Landscape in

Wild House Mouse (Mus musculus) Populations. *Mol Biol Evol* 2023; **40**(1): msac267.
45. McVean GA, Myers SR, Hunt S *et al.* The fine-scale structure of recombination rate variation in the human genome. *Science* 2004; **304**(5670): 581-584.
46. Auton A, Li YR, Kidd J *et al.* Genetic Recombination Is Targeted towards Gene Promoter Regions in Dogs. *Plos Genet* 2013; **9**(12): e1003984.
47. Lawal RA, Arora UP, Dumont BL. Selection shapes the landscape of functional variation in wild house mice. *Bmc Biol* 2021; **19**(1): 239.
48. Waters PD, Patel HR, Ruiz-Herrera A *et al.* Microchromosomes are building blocks of bird, reptile, and mammal chromosomes. *Proc Natl Acad Sci U S A* 2021; **118**(45): e2112494118.
49. Myers S, Bottolo L, Freeman C *et al.* A fine-scale map of recombination rates and hotspots across the human genome. *Science* 2005; **310**(5746): 321-324.
50. Shultz AJ, Sackton TB. Immune genes are hotspots of shared positive selection across birds and mammals. *Elife* 2019; **8**: e41815.
51. Beeson SK, Mickelson JR, McCue ME. Exploration of fine-scale recombination rate variation in the domestic horse. *Genome Res* 2019; **29**(10): 1744-1752.
52. Pan Z, Wang Y, Wang M *et al.* An atlas of regulatory elements in chicken: A resource for chicken genetics and genomics. *Sci Adv* 2023; **9**(18): eade1204.
53. Fuentes RR, de Ridder D, van Dijk ADJ *et al.* Domestication Shapes Recombination Patterns in Tomato. *Mol Biol Evol* 2022; **39**(1): msab287.
54. Li G, Figueiro HV, Eizirik E *et al.* Recombination-Aware Phylogenomics Reveals the Structured Genomic Landscape of Hybridizing Cat Species. *Mol Biol Evol* 2019; **36**(10): 2111-2126.
55. Li Y, Chen S, Rapakoulia T *et al.* Deep learning identifies and quantifies recombination hotspot determinants. *Bioinformatics* 2022; **38**(10): 2683-2691.
56. Quilodran CS, Montoya-Burgos JI, Currat M. Harmonizing hybridization dissonance in conservation. *Commun Biol* 2020; **3**(1): 391.
57. Ma Y, Wang J, Hu Q *et al.* Ancient introgression drives adaptation to cooler and drier mountain habitats in a cypress species complex. *Commun Biol* 2019; **2**: 213.
58. Zheng Z, Wang X, Li M *et al.* The origin of domestication genes in goats. *Sci Adv* 2020; **6**(21): eaaz5216.
59. Kim BY, Huber CD, Lohmueller KE. Deleterious variation shapes the genomic landscape of introgression. *PLoS Genet* 2018; **14**(10): e1007741.
60. Schumer M, Xu C, Powell DL *et al.* Natural selection interacts with recombination to shape the evolution of hybrid genomes. *Science* 2018; **360**(6389): 656-660.
61. Janousek V, Munclinger P, Wang L *et al.* Functional organization of the genome may shape the species boundary in the house mouse. *Mol Biol Evol* 2015; **32**(5): 1208-1220.
62. Martin SH, Davey JW, Salazar C *et al.* Recombination rate variation shapes barriers to introgression across butterfly genomes. *PLoS Biol* 2019; **17**(2): e2006288.
63. Dias-Alves T, Mairal J, Blum MGB. Loter: A Software Package to Infer Local Ancestry for a Wide Range of Species. *Mol Biol Evol* 2018; **35**(9): 2318-2326.
64. Browning SR, Waples RK, Browning BL. Fast, accurate local ancestry inference with FLARE. *Am J Hum Genet* 2023; **110**(2): 326-335.
65. Simons YB, Sella G. The impact of recent population history on the deleterious mutation load in humans and close evolutionary relatives. *Curr Opin Genet Dev* 2016; **41**: 150-158.
66. Ritz KR, Noor MAF, Singh ND. Variation in Recombination Rate: Adaptive or Not? *Trends Genet*

2017; **33**(5): 364-374.
67. Rees H, Dale PJ. Chiasmata and variability in Lolium and Festuca populations. *Chromosoma* 1974; **47**: 335–351.
68. Hufford MB, Xu X, van Heerwaarden J *et al.* Comparative population genomics of maize domestication and improvement. *Nat Genet* 2012; **44**(7): 808-811.
69. Sae-Lim P, Kause A, Lillehammer M *et al.* Estimation of breeding values for uniformity of growth in Atlantic salmon (Salmo salar) using pedigree relationships or single-step genomic evaluation. *Genet Sel Evol* 2017; **49**(1): 33.
70. Makumburage GB, Stapleton AE. Phenotype uniformity in combined-stress environments has a different genetic architecture than in single-stress treatments. *Front Plant Sci* 2011; **2**: 12.
71. Marand AP, Zhao H, Zhang W *et al.* Historical Meiotic Crossover Hotspots Fueled Patterns of Evolutionary Divergence in Rice. *Plant Cell* 2019; **31**(3): 645-662.
72. Lesecque Y, Glemin S, Lartillot N *et al.* The red queen model of recombination hotspots evolution in the light of archaic and modern human genomes. *PLoS Genet* 2014; **10**(11): e1004790.
73. Winckler W, Myers SR, Richter DJ *et al.* Comparison of fine-scale recombination rates in humans and chimpanzees. *Science* 2005; **308**(5718): 107-111.
74. Brunschwig H, Levi L, Ben-David E *et al.* Fine-scale maps of recombination rates and hotspots in the mouse genome. *Genetics* 2012; **191**(3): 757-764.
75. Sankararaman S, Mallick S, Dannemann M *et al.* The genomic landscape of Neanderthal ancestry in present-day humans. *Nature* 2014; **507**(7492): 354-357.
76. Pool JE. The Mosaic Ancestry of the Drosophila Genetic Reference Panel and the D. melanogaster Reference Genome Reveals a Network of Epistatic Fitness Interactions. *Mol Biol Evol* 2015; **32**(12): 3236-3251.
77. Corbett-Detig R, Nielsen R. A hidden markov model approach for simultaneously estimating local ancestry and admixture time using next generation sequence data in samples of arbitrary ploidy. *PLoS Genet* 2017; 13: e1006529.
78. Ai H, Fang X, Yang B, *et al*. Adaptation and possible ancient interspecies introgression in pigs identified by whole-genome sequencing. *Nat Genet* 2015; 47: 217-225.
79. Wang MS, Wang S, Li Y, *et al*. Ancient Hybridization with an unknown population facilitated high-altitude adaptation of canids. Mol Biol Evol 2020; 37: 2616-2629.
80. Bolger AM, Lohse M, Usadel B. Trimmomatic: a flexible trimmer for Illumina sequence data. *Bioinformatics* 2014; **30**(15): 2114-2120.
81. McKenna A, Hanna M, Banks E *et al.* The Genome Analysis Toolkit: A MapReduce framework for analyzing next-generation DNA sequencing data. *Genome Res* 2010; **20**(9): 1297-1303.
82. Purcell S, Neale B, Todd-Brown K *et al.* PLINK: A tool set for whole-genome association and population-based linkage analyses. *Am J Hum Genet* 2007; **81**(3): 559-575.
83. Chernomor O, von Haeseler A, Minh BQ. Terrace Aware Data Structure for Phylogenomic Inference from Supermatrices. *Syst Biol* 2016; **65**(6): 997-1008.
84. Zhang C, Dong SS, Xu JY *et al.* PopLDdecay: a fast and effective tool for linkage disequilibrium decay analysis based on variant call format files. *Bioinformatics* 2019; **35**(10): 1786-1788.
85. Danecek P, Auton A, Abecasis G *et al.* The variant call format and VCFtools. *Bioinformatics* 2011; **27**(15): 2156-2158.
86. Szpiech ZA, Hernandez RD. selscan: An Efficient Multithreaded Program to Perform EHH-Based Scans for Positive Selection. *Molecular Biology and Evolution* 2014; **31**(10): 2824-2827.

87. Martin SH, Davey JW, Jiggins CD. Evaluating the use of ABBA-BABA statistics to locate introgressed loci. *Mol Biol Evol* 2015; **32**(1): 244-257.
88. Price AL, Tandon A, Patterson N *et al.* Sensitive detection of chromosomal segments of distinct ancestry in admixed populations. *PLoS Genet* 2009; **5**(6): e1000519.
89. Kaur T, Rockman MV. Crossover heterogeneity in the absence of hotspots in Caenorhabditis elegans. *Genetics* 2014; **196**(1): 137-148.
90. De Maio FG. Income inequality measures. *J Epidemiol Community Health* 2007; **61**(10): 849-852.
91. Xiao-Ning Zhu, Yu-Zhe Wang, Chong Li *et al.* Chicken chromatin accessibility atlas accelerates epigenetic annotation of birds and gene fine-mapping associated with growth traits. *Zoological Research* 2023, **44**(1): 53-62.
92. Kolberg L, Raudvere U, Kuzmin I *et al.* g:Profiler-interoperable web service for functional enrichment analysis and gene identifier mapping (2023 update). *Nucleic Acids Res* 2023; **51**(W1): W207-W212.
93. Halldorsson BV, Palsson G, Stefansson OA *et al.* Characterizing mutagenic effects of recombination through a sequence-level genetic map. *Science* 2019; **363**(6430): 939-939.
94. Frazer KA, Ballinger DG, Cox DR *et al.* A second generation human haplotype map of over 3.1 million SNPs. *Nature* 2007; **449**(7164): 851-U853.
95. Bell AD, Mello CJ, Nemesh J *et al.* Insights into variation in meiosis from 31,228 human sperm genomes. *Nature* 2020; **583**(7815): 259-264.
96. Lange J, Yamada S, Tischfield SE *et al.* The Landscape of Mouse Meiotic Double-Strand Break Formation, Processing, and Repair. *Cell* 2016; **167**(3): 695-708.e16.
97. Baumdicker F, Bisschop G, Goldstein D *et al.* Efficient ancestry and mutation simulation with msprime 1.0. *Genetics* 2022; **220**(3): iyab229.

Figures:

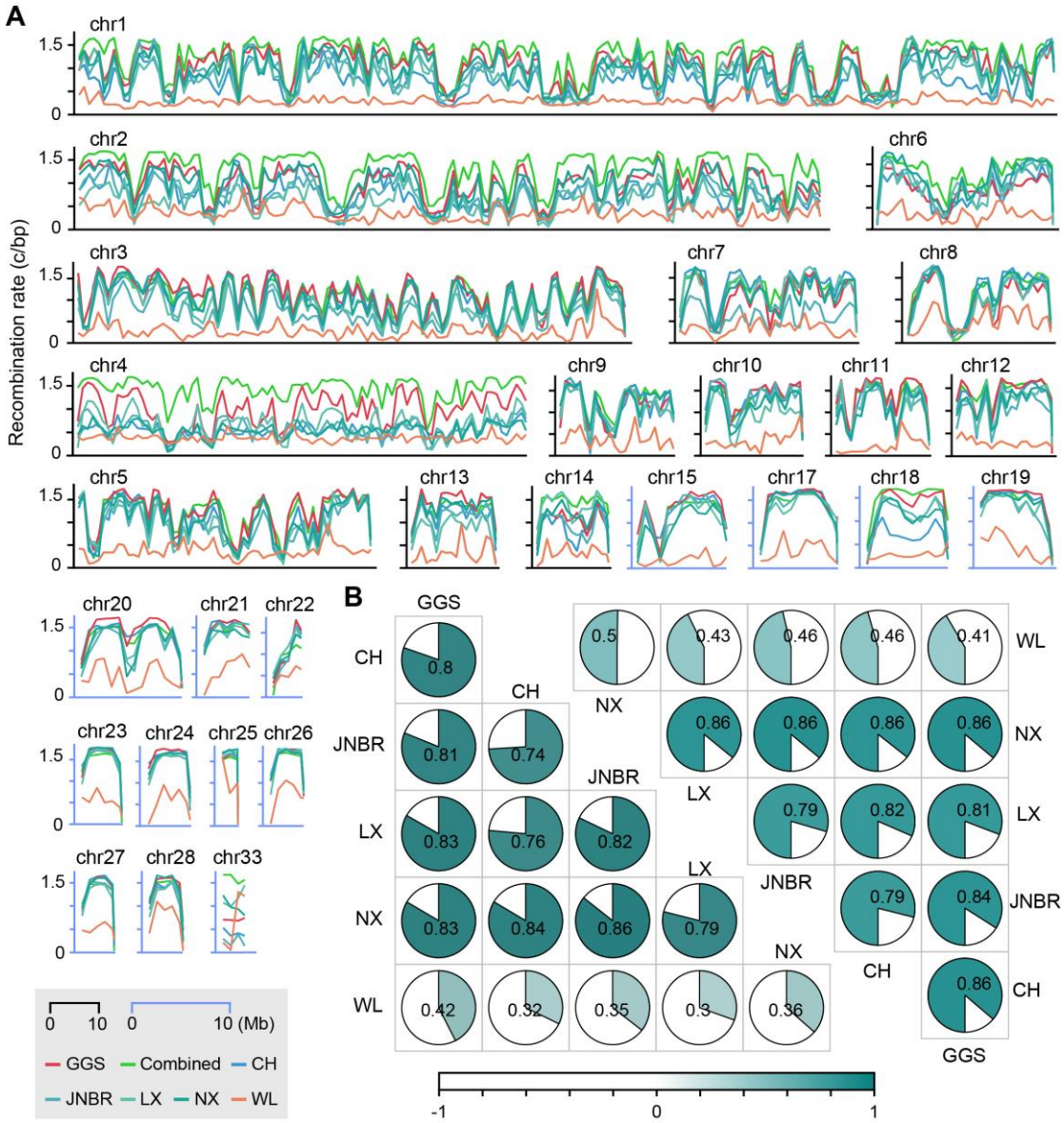

Fig 1. Landscape of recombination rates in GGS and domestic chickens. (A) The distribution of the recombination rate (c/bp). Estimates are normalized using 1-Mb sliding windows. (B) Pearson's rank correlation coefficient for the recombination rate for macrochromosomes (left) and microchromosomes (right) from each pair of populations. Macrochromosomes include chr1-5 and the rest are microchromosomes. Dot chromosomes were excluded from this analysis due to their limited length and high missing rate in variant calling. GGS, Gallus gallus spadiceus; CH, Chahua chicken; JNBR, Jining Bairi Chickens; LX, Luxi Fighting; NX, Nixi; WL, White Leghorn.

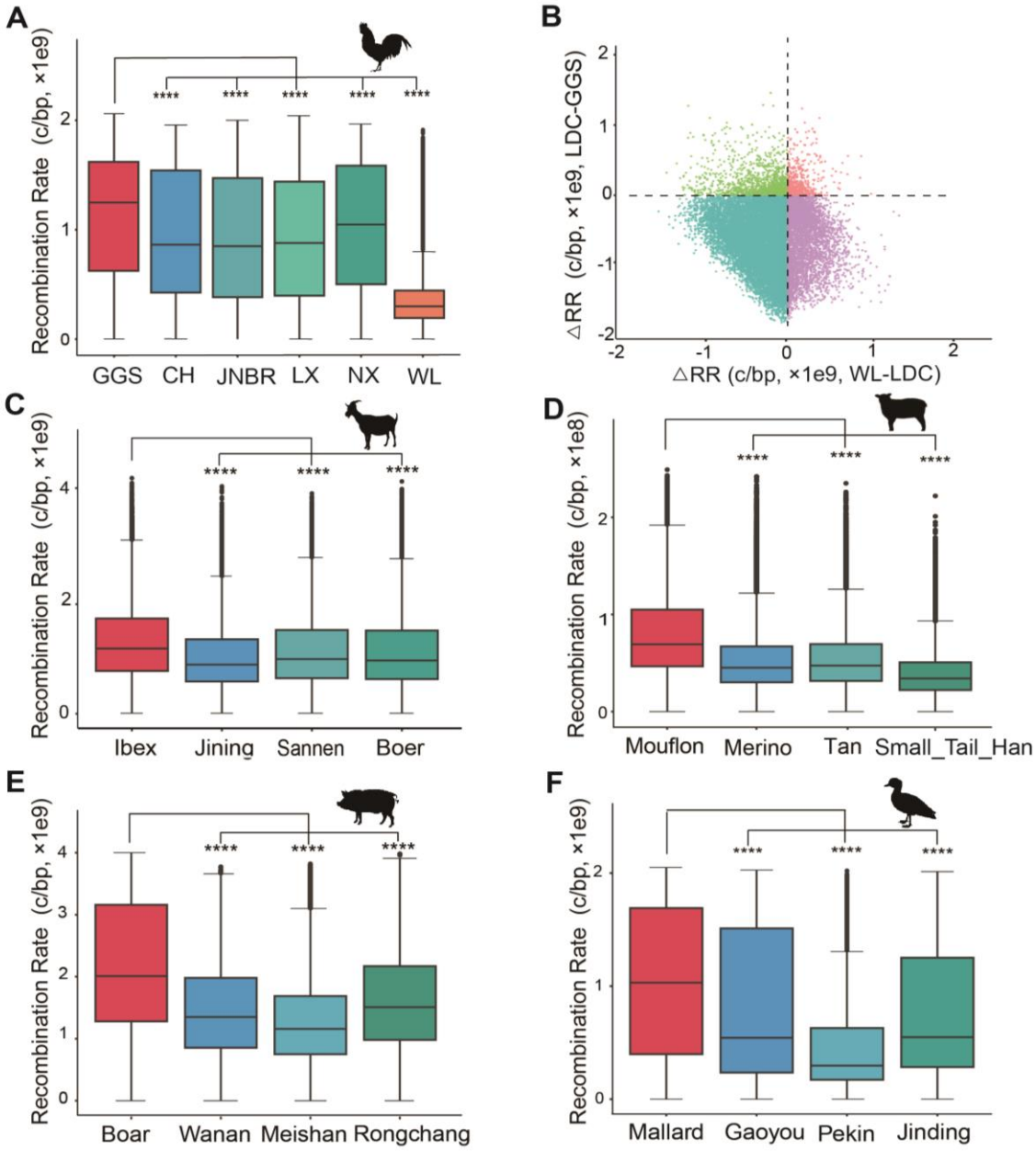

Fig 2. Recombination landscape between domesticated species and their wild relatives. (A) Recombination rates of Red Jungle Fowl (*Gallus gallus spadiceus*, GGS) and domesticated chickens. (B) The level of recombination rate (RR) changes in LDC and WL compared to GGS. (C) Recombination rates of Bezoar ibex (*Capra aegagrus*) and domesticated goats. (D) Recombination rates of mouflon (*Ovis gmelini*) and domestic sheep. (E) Recombination rates of Asian wild boar (*Sus scrofa*) and domestic pigs. (F) Recombination rates of mallard duck (*Anas platyrhynchos*) and domestic ducks. In this figure, **** indicate $P < 0.0001$ by the Wilcoxon test.

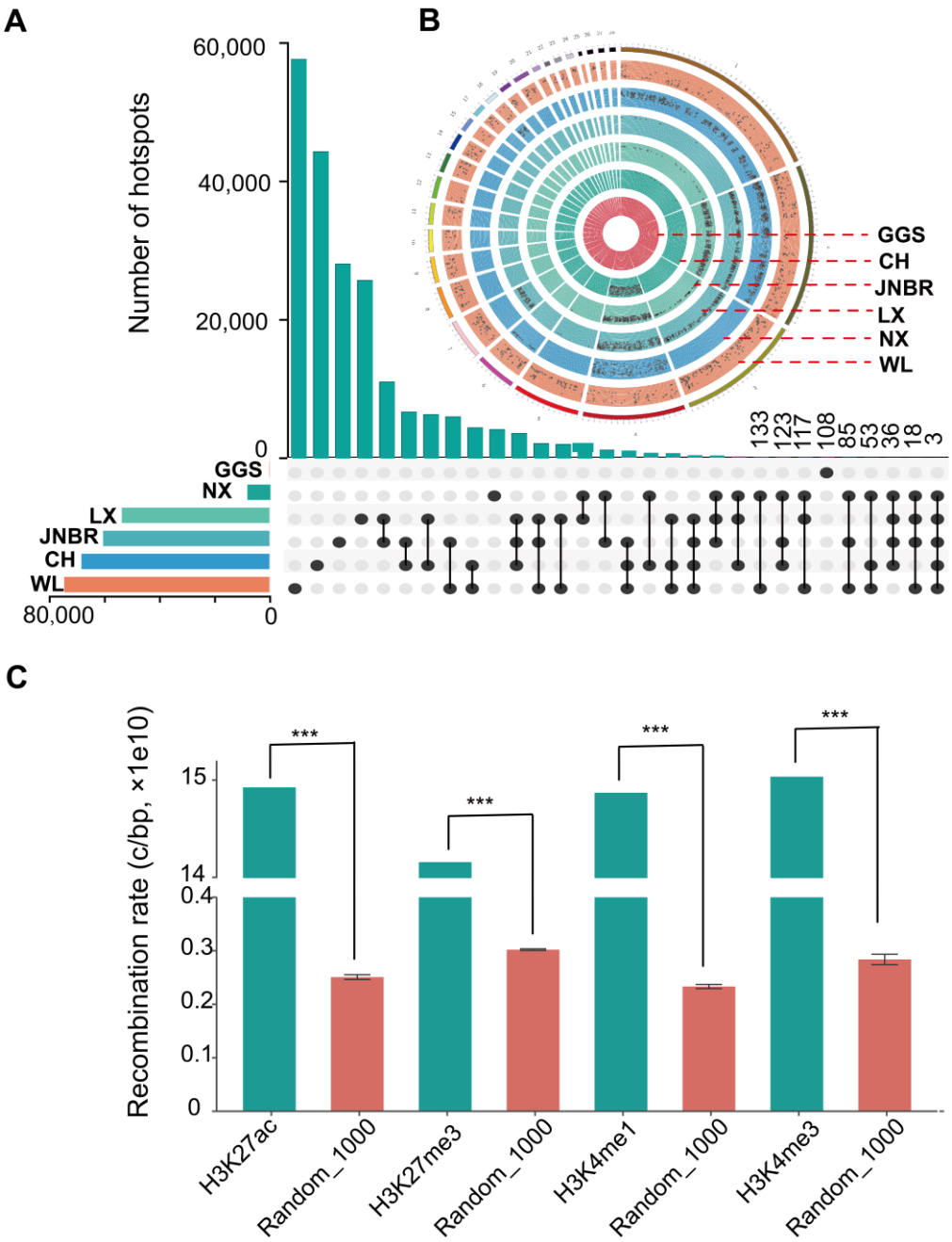

Fig 3. Recombination hotspots variation across genomes. (A) Identification of shared and breed-specific recombination hotspots in GGS and chickens. (B)The localization of recombination hotspots on each chromosome is depicted in concentric circles, with GGS, NX, LX, JNBR, CH, and WL represented from innermost to outermost circles. (C) Comparison of recombination rates between regions associated with four histone modifications (H3K27ac, H3K27me3, H3K4me1, and H3K4me3) and randomly selected regions (Random_1000, n=1000) of equal length from the rest of the genome. *** indicates $P < 0.001$ by one-sample t-test.

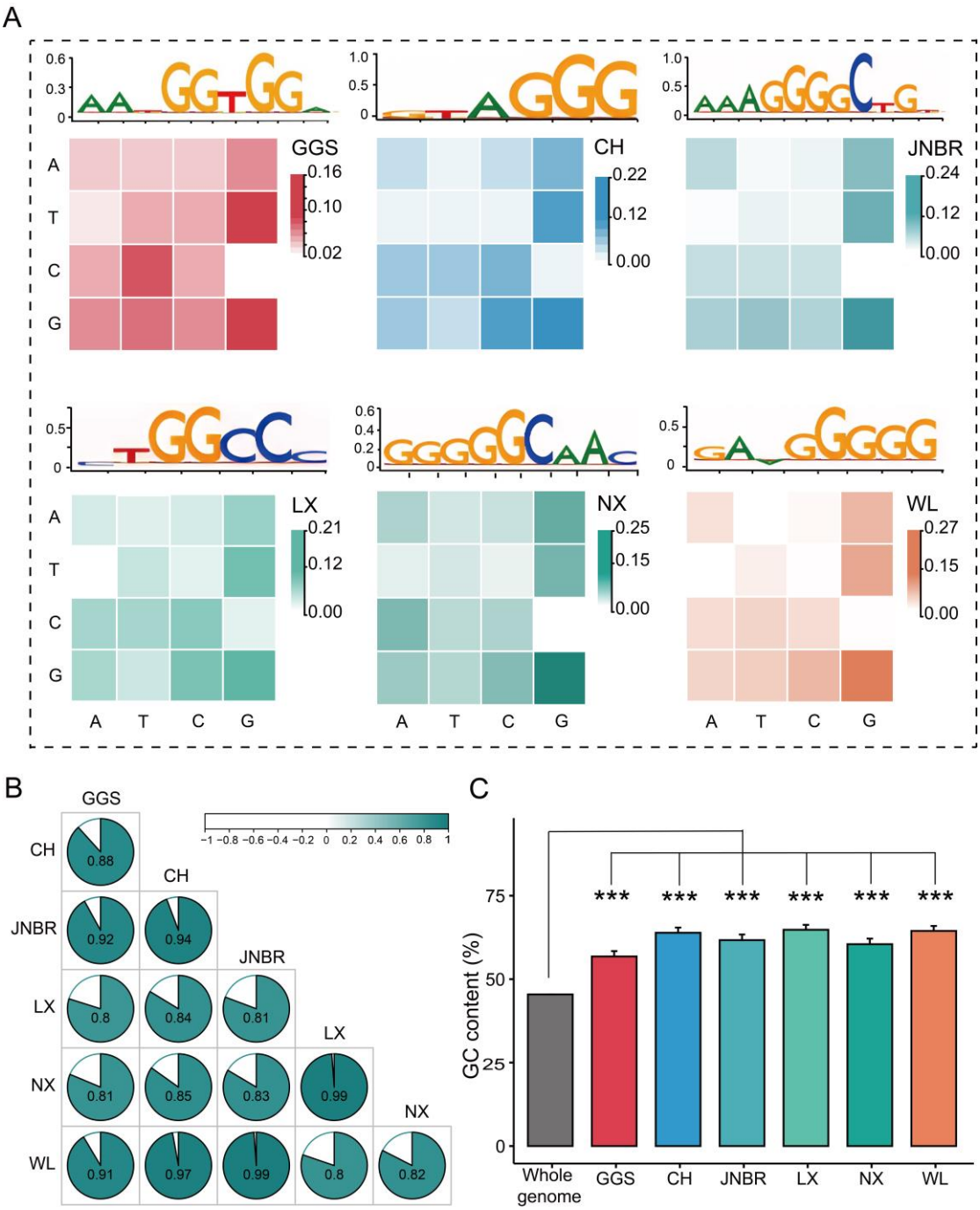

Fig 4. The distribution of the predicted motif for the recombination hotspot across different populations. (A) Results of the composite motif detected by RHSNet. The top shows the motif embeddings in each chicken population, and the bottom heatmap indicates the frequency of 2-mer occurrence in the detected motifs. (B) Pearson's correlation coefficients between the frequency of 2-mer motif between each pair of populations. (C) Average GC content in the whole genome and motif sequences. *** indicates $P < 0.001$ by one-sample t-test.

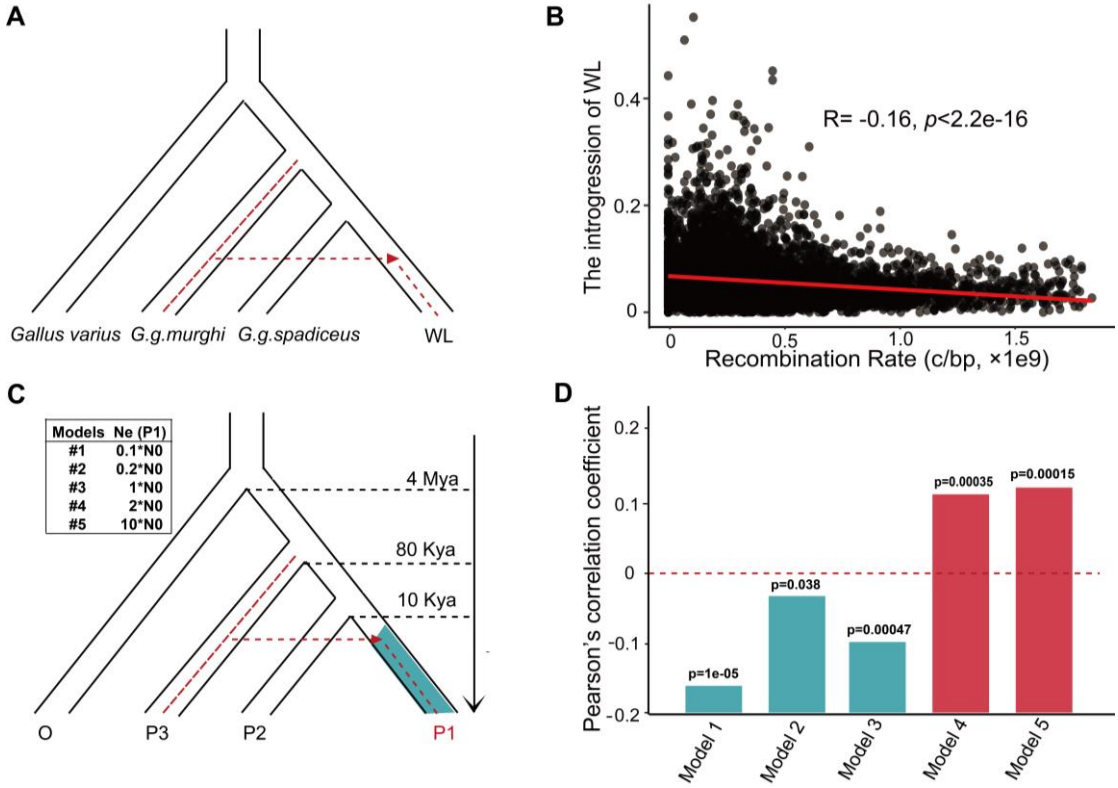

Fig 5. Correlation between introgression frequency and recombination rate. (A) The population topology for the detection of GGM introgressed regions in WL. (B) Correlation between the recombination rate and the frequency of introgression. (C) The topology for the four populations used in the simulations. In each of the five models, the population size for O, P3, P2 is set to N0, and the population size for P1 is set to 0.1*N0, 0.2*N0, N0, 2*N0, and 10*N0, respectively. (D) Pearson's correlation coefficients between the frequency of gene flow and the recombination rate under five models.